Real-Space Investigation of Structural Changes at the Metal-Insulator Transition in VO_2

Serena A. Corr*
School of Physical Sciences, University of Kent, Canterbury, Kent CT2 7NH, United Kingdom

Daniel P. Shoemaker, Brent C. Melot, and Ram Seshadri
Materials Department and Materials Research Laboratory, University of California, Santa Barbara, California, 93106, USA
(Received 4 June 2010; published 30 July 2010)

Synchrotron x-ray total scattering studies of structural changes in rutile VO_2 at the metal-insulator transition temperature of 340 K reveal that monoclinic and tetragonal phases of VO_2 coexist in equilibrium, as expected for a first-order phase transition. No evidence for any distinct intermediate phase is seen. Unbiased local structure studies of the changes in V-V distances through the phase transition, using reverse Monte Carlo methods, support the idea of phase coexistence and point to the high degree of correlation in the dimerized low-temperature structure. No evidence for short-range V-V correlations that would be suggestive of *local* dimers is found in the metallic phase.

DOI: 10.1103/PhysRevLett.105.056404 PACS numbers: 71.30.+h, 61.05.cf, 61.50.Ks

VO_2 undergoes a transition from a metal to a nonmagnetic insulator upon cooling below 340 K [1]. Accompanying this transition is a structural change from the high-temperature tetragonal phase to a low-temperature monoclinic phase, where pairing and tilting of vanadium ions result in chains with alternating long and short V-V distances along the c axis (Fig. 1) [2–4]. The mechanism underpinning the insulating behavior of the low-temperature phase continues to attract widespread interest, and recent work suggests the simultaneous role of the V-V pairing and electron correlation to drive the system from a correlated metal to a slightly less correlated insulator [5–7]. Diverse methods have been used to understand this transition, including recent probes of dynamics and techniques sensitive to spatial inhomogeneities [8–11]. The phenomenon as it occurs in nanostructures is also receiving increasing attention [12–14].

Above 340 K, the rutile VO_2 structure in space group $P4_2/mnm$ has a single near-neighbor V-V distance of 2.88 Å [15,16]. Below 340 K, the monoclinic structure in space group $P2_1/c$ is characterized by V-V dimers along the c axis displaying two distinct V-V distances: 2.65 and 3.12 Å [16–18]. The structures are displayed in Fig. 1. Interestingly, several recent papers address the formation of domainlike regions in monoclinic VO_2 on approaching the transition temperature from below [7,9,19,20]. An unresolved question regarding the nature of these domains is whether they are associated with an intermediate phase formed during the transition. A second question concerns the possible existence of dimers, albeit over short length scales, persisting in the metallic high-temperature phase.

Here we employ synchrotron x-ray total scattering in conjunction with real-space analysis—using least-squares as well as reverse Monte Carlo methods—to show that the transition from the low-temperature monoclinic to the high-temperature tetragonal phase in rutile VO_2 occurs in a first-order manner, with coexistence of the low- and high-temperature phases at the transition temperature. We employ pair distribution function (PDF) analysis, which has emerged in recent years as an indispensable tool for probing and understanding structural changes, and specifically, the range-dependence thereof [21–24]. The advantages of the PDF method lie in its ability to probe structural changes that lack long-range correlations, which are not captured by Bragg peaks in x-ray or neutron scattering. By analyzing PDF data with large-box reverse Monte Carlo (RMC) simulations, we are able to produce a supercell where the local environment is free from symmetry constraints of the high- or low-temperature structures [25–27]. Atomic positions can therefore relax to best fit the experimental data, which includes both the Bragg and diffuse components. This approach provides an opportunity to observe any continuum of atomic positions which might exist across the metal-to-insulator transition in VO_2.

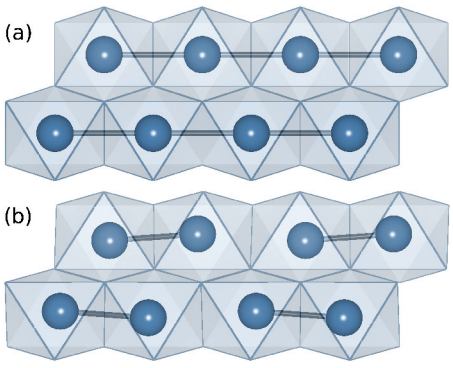

FIG. 1 (color online). (a) The metallic high-temperature tetragonal rutile form of VO_2 with a single V-V distance and (b) the insulating low-temperature monoclinic form, showing dimerized chains of alternating short and long V-V distances along the c axis.

Phase pure VO_2 powders were prepared in evacuated and sealed silica ampoules from a stoichiometric mixture of V_2O_5 (99.9%, Alfa Aesar) and V_2O_3, the latter obtained by reduction of V_2O_5 in 5% H_2/N_2 gas at 900 °C. Synchrotron total scattering data on powders in Kapton tubes were collected in transmission mode at beam line 11-ID-B of the Advanced Photon Source at Argonne National Laboratory by using x rays with energies near 90 keV (wavelength $\lambda = 0.137\,02$ Å). Samples were heated and cooled continuously from 250 to 400 K at a rate of 50 K h^{-1} using an Oxford Cryosystems Cryostream 700. Scattering data were collected on an image plate system with a sample-to-detector distance of 250 mm. Raw images were processed using FIT2D [28]. PDFs were extracted as $G(r)$ using PDFGETX2 with $Q_{max} = 25$ Å^{-1} [29]. Least-squares profile refinements were carried out using PDFGUI [30]. RMC simulations were performed using RMCPROFILE [31] with a $10 \times 10 \times 16$ supercell, starting from atomic positions of the tetragonal structure. The simulations were constrained by the PDF [where $G(r)$ above corresponds to $D(r)$ as described by Keen [32]] up to $r = 25$ Å. RMC results shown in this work are averages of many simulations to ensure an unbiased representation of the fit to data.

Least-squares refinements to all the PDFs at 2 K intervals were performed using both monoclinic and tetragonal structures [Figs. 2(a) and 2(b), respectively]. In the case of data fit to a monoclinic structure [Fig. 2(a)], we obtain a good fit from $T = 250$ to 338 K. The high-temperature tetragonal structure [Fig. 2(b)] results in a good fit to the data from $T = 342$ to 400 K. The PDFs of the two structures are markedly different, as seen in Figs. 2(a) and 2(b). There are no significant changes (other than lattice constants) in either end member until the transition is reached. The sudden structural transition at $T = 340$ K is evident in plots of the goodness-of-fit parameters R_w to the high- and low-temperature structures as seen in Fig. 2(c). In addition to locating the transition itself, the evolution in both temperature regimes suggests pure, single-phase polymorphs of the VO_2 end members. There is no broad hysteresis in the transition because the measurement allows thermal equilibrium to be reached at each point. In addition, the sample is a bulk powder of large crystallites, which implies the possibility of many concurrent nucleation events.

Dimerization of the V cations leads to splitting of the 2*a* Wyckoff site in the tetragonal VO_2 structure. If a dimerized structure is fit using the high-temperature model, the structural changes must be accommodated by an increase in the V atomic displacement parameters U_{ij}, which could convey information of the directionality of the displacement. Figure 3(a) shows the least-squares refined values of the U_{ij} parameters of the tetragonal structure over the full temperature range. At all temperatures, $U_{11} \equiv U_{22}$ by symmetry. Above the transition, U_{33} is equal to U_{11}, while U_{12} (the only nondiagonal parameter allowed by symmetry) is negligible. The high-temperature V position is therefore spherical, and is shown on the right in Fig. 3(a). Below 340 K, dimerization along the *c* direction leads to a large increase in U_{33}. Tilting of V-V vectors off the *c* axis (zero above the transition) produces an increase in U_{12}. The

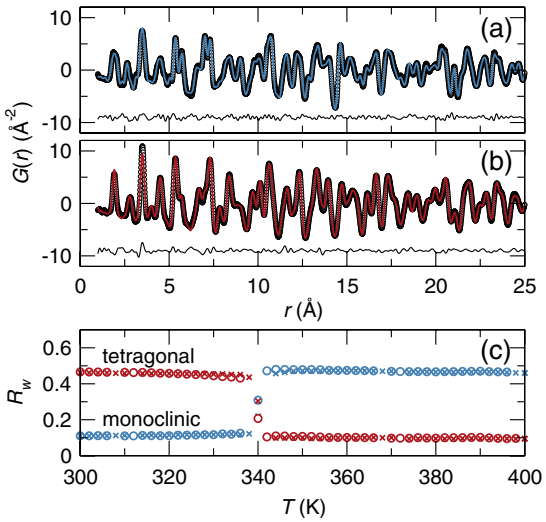

FIG. 2 (color online). Least-squares fits to the PDF of bulk VO_2 using (a) the low-temperature monoclinic structure for $T = 300$ K (R_w, 11.6%) and (b) the high-temperature tetragonal structure for $T = 400$ K (R_w, 9.6%). Circles are experimental data and lines are fits to the average structure. The difference is displayed below each fit. (c) Changes in the R_w fitting parameters, shown for cooling (○) and heating (×) through the transition temperature, show an abrupt transition with good fits at all temperatures outside of $T = 340$ K.

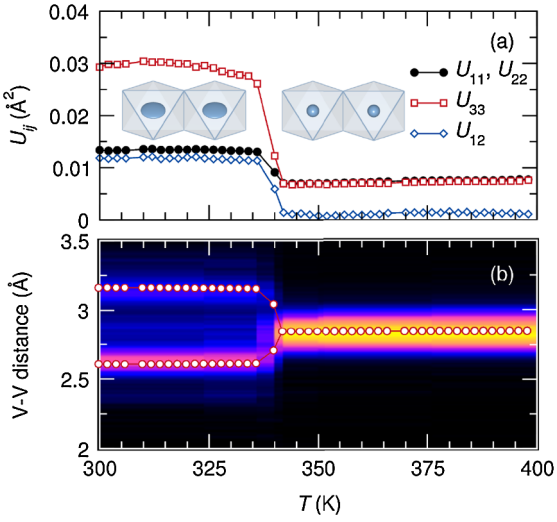

FIG. 3 (color online). (a) Thermal parameters (U_{ij}) obtained from PDF least-squares refinement as a function of temperature reveal abrupt changes at the transition temperature. Thermal ellipsoids (99%) for neighboring V polyhedra in the *c* direction are shown above and below the transition temperature. (b) V-V bond distances from the least-squares refinement (points) overlaid with a map of the V-V distances obtained from RMC modeling.

corresponding growth and elongation of the V thermal ellipsoids are seen on the left in Fig. 3(a).

The split V positions and corresponding dimerized V-V distances are the hallmark of cooling through the transition, and we use the PDF to extract the distances directly. If there were a gradual shift in V-V distances over the extent of a wide transition region, which other probes such as the electrical resistivity suggest, the local structure information in the PDF would reproduce these distances regardless of whether or not they are correlated over long ranges. Least-squares refinements of the V-V distances (using the appropriate monoclinic or tetragonal model for each structure) are displayed as points in Fig. 3(b) and show an abrupt change upon cooling through the transition. The distances at 336 and 342 K are effectively unchanged from the low- and high-temperature structures at 300 and 400 K, respectively, so the structural transition occurs within this range ($\Delta T < 6$ K). The least-squares refinements, however, are predicated on the choice of a monoclinic or tetragonal unit cell.

Histograms of V-V distances from RMC supercells (not constrained by symmetry) are displayed as an intensity map in Fig. 3(b). They display excellent agreement with the least-squares refined values for all points except $T =$ 340 K, implying that the single-phase least-squares refinements accurately reproduce the true distribution of V-V distances in the end members. However, at $T = 340$ K the least-squares refined distances are of intermediate length, while the RMC V-V histogram is unclear. Is there an intermediate phase with V-V distances that are distinct from the monoclinic and tetragonal structures, or is there a mixture of two phases? Our subsequent analysis of the linear combination of experimental PDFs, along with V positions from RMC simulations, can resolve this issue.

In Fig. 4(a), experimental PDFs are displayed for $T =$ 334, 340, and 342 K: below, during, and above the structural transition temperature. The $T = 334$ and 342 K PDFs can be refined to the end-member structures, so a linear combination of these two PDFs produces a two-phase PDF containing three V-V distances: two monoclinic and one tetragonal. This linear combination PDF is displayed as the points behind the $T = 340$ K data, and tracks the data up to 25 Å. The difference curve between the combination PDF and the $T = 340$ K data is shown in Fig. 4(b), showing that the two PDFs are identical within the limits of experimental noise. The agreement implies that, even on a local scale, the VO_2 sample at 340 K comprises two structurally distinct regions, corresponding directly to the tetragonal or the monoclinic structures. No additional contribution to the PDF is found.

Corroborating evidence for the two-phase combination is seen in RMC simulations. We examine the distribution of V positions around the ideal crystallographic site in real space by folding the positions of all V in the RMC supercell back into a single unit cell, which produces a cloud of

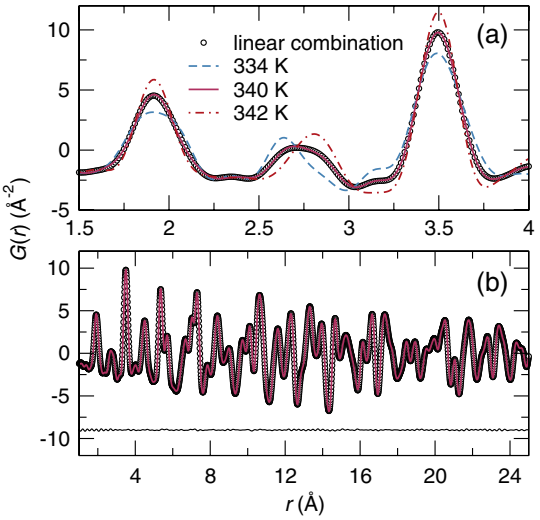

FIG. 4 (color online). (a) Experimental x-ray PDFs from VO_2 at T below (334 K), equal to (340 K), and above (342 K) the transition temperature. A linear combination of the 334 and 342 K data is shown as points, along with a difference curve to the 340 K data. In (b) the full fitting range is shown—at the transition temperature the sample is comprised of two distinct end-member phases.

1600 V positions (from a $10 \times 10 \times 16$ supercell) on each site. This cloud is viewed as a two-dimensional histogram showing the most probable positions of V cations in the a-c plane in Fig. 5. For each cloud with $T > 340$ K, V distributions are spherical [as seen in the ellipsoids in Fig. 3(a)] and centered on the ideal tetragonal positions. For $T <$ 340 K, dramatic splitting of the V position is seen. These two spots correspond to the end-member monoclinic positions. We see no evolution of V clouds versus temperature far from the transition, but the 340 K cloud possesses an

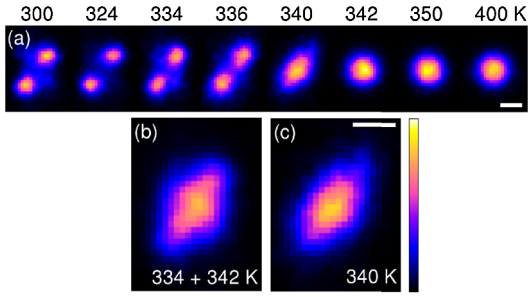

FIG. 5 (color online). (a) The relative probabilities of V atom positions as obtained from RMC modeling are dimerized at four temperatures below and spherical at three temperatures above the transition. At $T = 340$ K, the probability distribution is intermediate. In (b), a two-phase model is formed by averaging the experimental maps from $T = 334$ and 342 K, both of which resemble the low- and high-temperature end members. This resulting map appears similar to the 340 K data reproduced in (c). Scale bars are 0.2 Å. The color bar indicates minimum and maximum probability.

intermediate shape, distinct from the two regimes on either side. Just as was performed for the experimental PDFs themselves, we can linearly combine RMC results to produce models of a 1:1 mixture of the two phases. In Fig. 5(b), an average of the clouds from 334 and 342 K is displayed, as a model of coexistence of the end members. The experimental cloud from $T = 340$ K is reproduced in Fig. 5(c), and their similar appearance indicates that this is a two-phase mixture, in agreement with the linear combinations of the PDF in Fig. 4.

Qazilbash *et al.* [9] have recently suggested the formation of ''metallic nanopuddles'' at the transition temperature, and Cava and co-workers [7] have suggested the importance of metal-metal dimers in a series of substituted $V_{1-x}M_xO_2$ (M = Nb, Mo) samples. What has not been clear up to now is whether these implied a third, intermediate phase of VO_2. Here, we have shown that at the transition temperature there are only two distinct phase populations: low-temperature monoclinic VO_2 together with the high-temperature tetragonal phase. Above the transition, there is no evidence for the presence of V-V dimers.

It is a pleasure to acknowledge R. J. Cava for suggestions and encouragement, and P. J. Chupas and K. W. Chapman for assistance with data collection at APS beam line 11-ID-B, supported by the DOE Office of Basic Energy Sciences under Contract No. W-31-109-Eng.-38. S. A. C. acknowledges research support from the University of Kent. We received support from the LANL-UCSB Institute for Multiscale Materials Studies and the NSF through Grant No. DMR 0449354 to R. S. and MRSEC facilities (Grant No. DMR 0520415). RMC simulations were performed using computational resources of the California NanoSystems Institute, supported in part by Hewlett-Packard.

*s.a.corr@kent.ac.uk

[1] F. J. Morin, Phys. Rev. Lett. **3**, 34 (1959).
[2] J. B. Goodenough, Phys. Rev. **117**, 1442 (1960).
[3] C. N. Berglund and H. J. Guggenheim, Phys. Rev. **185**, 1022 (1969).
[4] A. Zylbersztejn and N. F. Mott, Phys. Rev. B **11**, 4383 (1975).
[5] M. Imada, A. Fujimori, and Y. Tokura, Rev. Mod. Phys. **70**, 1039 (1998).
[6] J. M. Tomczak, F. Aryasetiawan, and S. Biermann, Phys. Rev. B **78**, 115103 (2008).
[7] K. L. Holman, T. M. McQueen, A. J. Williams, T. Klimczuk, P. W. Stephens, H. W. Zandbergen, Q. Xu, F. Ronning, and R. J. Cava, Phys. Rev. B **79**, 245114 (2009).
[8] A. Cavalleri, M. Rini, H. H. W. Chong, S. Fourmaux, T. E. Glover, P. A. Heimann, J. C. Kieffer, and R. W. Schoenlein, Phys. Rev. Lett. **95**, 067405 (2005).
[9] M. M. Qazilbash *et al.*, Science **318**, 1750 (2007).
[10] S. Shin, S. Suga, M. Taniguchi, M. Fujisawa, H. Kanzaki, A. Fujimori, H. Daimon, Y. Ueda, K. Kosuge, and S. Kachi, Phys. Rev. B **41**, 4993 (1990).
[11] P. Baum, D.-S. Yang, and A. H. Zewail, Science **318**, 788 (2007).
[12] S. A. Corr, M. Grossman, J. D. Furman, B. C. Melot, A. K. Cheetham, K. R. Heier, and R. Seshadri, Chem. Mater. **20**, 6396 (2008).
[13] J. I. Sohn, H. J. Joo, D. Ahn, H. H. Lee, A. E. Porter, K. Kim, D. J. Kang, and M. E. Welland, Nano Lett. **9**, 3392 (2009).
[14] S. Zhang, J. Y. Chou, and L. J. Lauhon, Nano Lett. **9**, 4527 (2009).
[15] D. B. McWhan, M. Marezio, J. P. Remeika, and P. D. Dernier, Phys. Rev. B **10**, 490 (1974).
[16] B. Poumellec, J. F. Marucco, and B. Touzelin, Phys. Rev. B **35**, 2284 (1987).
[17] G. Andersson, Acta Chem. Scand. **10**, 623 (1956).
[18] C. Leroux, G. Nihoul, and G. Van Tendeloo, Phys. Rev. B **57**, 5111 (1998).
[19] H. S. Choi, J. S. Ahn, J. H. Jung, T. W. Noh, and D. H. Kim, Phys. Rev. B **54**, 4621 (1996).
[20] H.-T. Kim, Y. W. Lee, B.-J. Kim, B.-G. Chae, S. J. Yun, K.-Y. Kang, K.-J. Han, K.-J. Yee, and Y.-S. Lim, Phys. Rev. Lett. **97**, 266401 (2006).
[21] X. Qiu, T. Proffen, J. F. Mitchell, and S. J. L. Billinge, Phys. Rev. Lett. **94**, 177203 (2005).
[22] V. Petkov, Mater. Today **11**, 28 (2008).
[23] P. J. Chupas, S. Chaudhuri, J. C. Hanson, X. Qiu, P. L. Lee, S. D. Shastri, S. J. L. Billinge, and C. P. Grey, J. Am. Chem. Soc. **126**, 4756 (2004).
[24] K. Page, T. Kolodiazhnyi, T. Proffen, A. K. Cheetham, and R. Seshadri, Phys. Rev. Lett. **101**, 205502 (2008).
[25] A. L. Goodwin, S. A. T. Redfern, M. T. Dove, D. A. Keen, and M. G. Tucker, Phys. Rev. B **76**, 174114 (2007).
[26] D. P. Shoemaker, J. Li, and R. Seshadri, J. Am. Chem. Soc. **131**, 11 450 (2009).
[27] D. P. Shoemaker, R. Seshadri, A. L. Hector, A. Llobet, T. Proffen, and C. J. Fennie, Phys. Rev. B **81**, 144113 (2010).
[28] A. P. Hammersley, ESRF Internal Report No. ESRF97HA02T, 1997.
[29] X. Qiu, J. W. Thompson, and S. J. L. Billinge, J. Appl. Crystallogr. **37**, 678 (2004).
[30] C. L. Farrow, P. Juhás, J. W. Liu, D. Bryndin, E. S. Božin, J. Bloch, T. Proffen, and S. J. L. Billinge, J. Phys. Condens. Matter **19**, 335219 (2007).
[31] M. G. Tucker, D. A. Keen, M. T. Dove, A. L. Goodwin, and Q. Hui, J. Phys. Condens. Matter **19**, 335218 (2007).
[32] D. A. Keen, J. Appl. Crystallogr. **34**, 172 (2001).